A recombinant receptor-binding domain in trimeric form generates completely protective immunity against SARS-CoV-2 infection in nonhuman primates

Limin Yang[1]*†, Deyu Tian[2]*, Jian-bao Han[4]*, Wenhui Fan[1], Yuan Zhang[1], Yunlong Li[1], Wenqiang Sun[2], Yanqiu Wei[1], Xiaodong Tian[2], Dan-dan Yu[3,4], Xiao-li Feng[4], Gong Cheng[5,6]†, Yong-tang Zheng[3,4]†, Yuhai Bi[1,2]†, Wenjun Liu[1,2,4]†

[1] CAS Key Laboratory of Pathogenic Microbiology and Immunology, Institute of Microbiology, Center for Influenza Research and Early Warning (CASCIRE), CAS-TWAS Center of Excellence for Emerging Infectious Diseases (CEEID), Chinese Academy of Sciences, Beijing 100101, China

[2] University of Chinese Academy of Sciences, Beijing 101408, China

[3] Key Laboratory of Animal Models and Human Disease Mechanisms of the Chinese Academy of Sciences, Kunming Institute of Zoology, Chinese Academy of Sciences, Kunming, Yunnan 650223, China

[4] Kunming National High-Level Biosafety Research Center for Nonhuman Primates, Center for Biosafety Mega-Science, Kunming Institute of Zoology, Chinese Academy of Sciences, Kunming, Yunnan 650107, China

[5] Institute of Infectious Diseases, Shenzhen Bay Laboratory, Shenzhen, Guangdong, 518000, China

[6] Tsinghua-Peking Center for Life Sciences, School of Medicine, Tsinghua University, Beijing, 100084, China

* These authors contributed equally to this work.

† Corresponding authors. E-mail: liuwj@im.ac.cn (W.L.); lmyang@im.ac.cn (L.Y.); beeyh@im.ac.cn (Y.B.); gongcheng@mail.tsinghua.edu.cn (G.C.); zhengyt@mail.kiz.ac.cn (Y.Z.)

Abstract

Safe and effective vaccination is critical to combatting the COVID-19 pandemic. Here, we developed a trimeric SARS-CoV-2 receptor-binding domain (RBD) subunit vaccine candidate that simulates the natural structure of the spike (S) trimer glycoprotein. Immunization with RBD-trimer induced robust humoral and cellular immune responses and a high level of neutralizing antibodies that were maintained for at least 4 months. Moreover, the antibodies that were produced in response to the vaccine effectively neutralized the SARS-CoV-2 501Y.V2 variant. Of note, when the titers of the antibodies dropped to a sufficiently low level, only one boost quickly activated the anamnestic immune response, resulting in complete protection against the SARS-CoV-2 challenge in *rhesus macaques* without typical histopathological changes or viral replication in the lungs and other respiratory tissues. Our results indicated that immunization with SARS-CoV-2 RBD-trimer could raise long-term and broad immunity protection in nonhuman primates, thereby offering an optimal vaccination strategy against COVID-19.

Keywords: COVID-19, SARS-CoV-2, receptor-binding domain, subunit vaccine, NHPs, variants

Introduction

Since severe acute respiratory syndrome coronavirus 2 (SARS-CoV-2) was identified as the causative agent for the current coronavirus disease (COVID-19) [1], the ongoing global pandemic has infected more than 1.6% (over 120 million people) of the world's population, which has caused a severe economic burden and hindered social development across the globe. There is an urgent need to develop safer and more effective vaccines to end the current health crisis. Researchers worldwide are racing to develop COVID-19 vaccines; more than 200 vaccine candidates are in development, and 70 are in clinical trials. Multiple vaccine development strategies have been pursued simultaneously, including viral vectors[2-4], inactivated whole viruses[5, 6], DNA[7, 8], RNA[9-11], subunits[12, 13], virus-like particles[14], and live attenuated viruses (World Health Organization, WHO). Vaccines with different development strategies have distinct advantages and application limitations. Therefore, the development of new vaccine strategies to avoid shortcomings is still the focus of vaccine researchers.

SARS-CoV-2 is a member of the *Betacoronavirus* genus of the *Coronaviridae* family of enveloped RNA viruses homologous to SARS and Middle East respiratory syndrome (MERS) coronaviruses. The viral surface spike (S) glycoprotein mediates receptor binding and cell entry and is the primary target for vaccine design[15]. To mimic the native S trimer structure, an artificially designed S trimer was constructed by fusing the C-terminal region of human type Iα collagen, and this construct was used for vaccine research[16]. Previous studies have found that both SARS-CoV and MERS-CoV display

antibody-dependent enhancement (ADE), leading to a potential risk of vaccine enhancement of disease[17, 18]. The principle is that the nonneutralizing antibodies produced in response to the vaccine mediate virus infection via the Fcγ receptor[18]. Considering the high degree of homology of SARS-CoV-2, the potential ADE effect needs to be considered seriously in designing COVID-19 vaccines. To mitigate the ADE effect, minimizing nonneutralizing epitopes and keeping only the critical neutralizing epitope to elicit robust protective immunity is a solution[19]. The receptor-binding domain (RBD) located at the C-terminus of the S1 subunit has thus attracted attention. Several lines of evidence have indicated that RBD-specific antibodies could minimize the ADE effect[20], and most discovered potent neutralizing antibody (NAb) target the RBD region[21, 22]. SARS-CoV-2 initiates viral replication by binding via the RBD to the cell surface receptor angiotensin-converting enzyme 2 (ACE2). Hence, the RBD can be used as a vaccine target to block viral attachment. Additionally, the RBD possesses T cell epitopes, which can provoke antiviral T cell responses[11, 12]. However, the molecular weight of the RBD is small, which leads to its weak immunogenicity. Some researchers have tried to express it by fusion with the Fc domain and prepare it as a dimer, thereby greatly enhancing its immunogenicity[13]. Some evidence has shown that the NAb level in SARS-CoV-2-infected humans significantly declines from the second month and can even be lost [23], allowing them to be reinfected [24]. This short-lasting antibody protection poses a severe challenge for vaccine development. In addition, SARS-CoV-2 is characterized by a high mutation rate, and some evidence has proven that the 501Y.V2 variant (B.1.351) that emerged in South Africa severely

reduced the protective efficacy of licensed mRNA vaccines [25-27]. Therefore, a vaccine strategy that can produce persistent and broad protection is particularly important.

In the present study, we designed and developed an RBD trimer as a candidate SARS-CoV-2 subunit vaccine. A single immunization elicited the acute production of protective NAbs in all *rhesus macaques*. Boost immunization induced a robust immune response, and a high titer of NAbs and a potent CD4 and CD8 T cell immune response were developed. The immune protection period lasted for at least four months (Neutralization titer > 100). Moreover, booster immunization could immediately activate the memory immune response, allowing an immunized individual to regain immune protection quickly. In addition, the vaccine-induced antibodies also had good neutralizing activity against the 501Y.V2 variant. Our vaccine candidate conferred significant protection and sterilizing immunity in vaccinated nonhuman primate lung tissue against SARS-CoV-2 infection.

Materials and Methods

Ethical statement

The protocols of all animal experiments were approved by Kunming National High-level Biosafety Research Center for Non-human Primates, Center for Biosafety Mega-Science, Kunming Institute of Zoology, Chinese Academy of Sciences (CAS) (permission number: IACUC20026) and performed according to the Animal Experimentation Guidelines. All applicable institutional and/or national guidelines for the care and use of animals were followed.

Animals

Five Chinese-origin male rhesus macaques *(Macaca mulatta*, animal numbers: #140829, #140271, #163957, # 17361, #17321) weighing 4.1 to 8.7 kg and aged 3 to 6 years old were obtained from the Institute of Beijing Xieerxin Biology Resource Co., Ltd. The animals were in acceptable physical condition and were free of clinical signs of any infection. During the study period, the animals were housed individually and monitored daily for signs of illness and distress.

Cell lines and virus

African green monkey kidney epithelial cells (Vero-E6) (ATCC, no. 1586) were used for SARS-CoV-2 virus propagation and NAb determination. The SARS-CoV-2 strain used in this experiment was provided by Kunming Institute of Zoology, Chinese Academy of Sciences (Kunming, China). The virus NMDC accession number is NMDCN0000HUI; the isolation strain is 20SF107, which was isolated and titrated in Vero-E6 cells.

Gene construction and protein generation

The RBD region (residues Ser_{325} – Ser_{530}) of the SARS-CoV-2 S protein (accession No. MN908947) was fused with an interleukin-10 signal peptide (accession No. CAG46825) at the N-terminus and foldon sequence (GYIPEAPRDGQAYVRKDGEWVLLSTFL) at the C-terminus to trimerize the protein. A C-terminal 6×His tag was also added to facilitate purification. The designed gene was synthesized by GenScript (Nanjing, China) using a mammalian codon-optimized sequence for enhanced expression and then cloned into the mammalian expression vector pCDNA3.4 (Thermo Fisher, USA) under the control of the CMV promoter. The fused protein was expressed in transfected HEK293 cells and secreted into the cell culture medium. After 72 h of culture, supernatants were harvested and purified by Ni-NTA affinity chromatography and gel filtration (Superdex 200, GE Healthcare, USA) and eluted in PBS (pH 7.2). Purified proteins were then analyzed by SDS-PAGE and Western blotting under both nonreducing and reducing conditions.

Immunization

For the vaccination group, three rhesus macaques were vaccinated three times by the i.m. route in the deltoid muscle with a total volume of 1 ml of vaccine formulation containing 50 μg of RBD-trimer admixed with AddaVax adjuvant (InvivoGen) at weeks 0, 3, and 21, as scheduled. Blood was collected from the femoral vein into 5 ml venoject II vacuum blood collection tubes containing citric acid to evaluate the immune response. For the sham vaccination group, two macaques were vaccinated i.m. with equal amounts of PBS replacing the candidate vaccine. Serum was obtained by centrifugation

145 at 1,200 × g at 4°C for 30 min, incubated at 56°C for 30 min, and inactivated by UV
146 irradiation at 254 nm for 10 min before use.

147 Challenge

148 Infectious work was performed in the Animal Biosafety Level 3 (ABSL-3) laboratory
149 at the Kunming National High-Level Biosafety Research Center for Non-Human
150 Primates, Kunming Institute of Zoology, Chinese Academy of Sciences (Kunming,
151 China). Five rhesus macaques were intratracheally (60%) and intranasally (40%; 20%
152 per naris) challenged with 1×10^7 $TCID_{50}$ of the virulent COVID-19 20SF107 strain 9
153 days after the final immunization. Rhesus macaques were monitored daily after the
154 challenge, and their health conditions, including appetite, water drinking, behavior,
155 appearance, and feces appearance, were recorded. When macaques showed severe
156 clinical symptoms and became moribund, they were promptly euthanized.

157 Necropsy and macroscopic pathology

158 Animals were euthanized one week after the challenge, and necropsies were performed
159 in the ABSL-3 facility. Macroscopic features of necropsied tissues of the macaques
160 were observed at dissection. For histopathology and immunohistochemistry analyses,
161 nasal mucosa, trachea, lung, liver, spleen and kidney tissue samples collected from each
162 animal were fixed by immersion in 4% neutral-buffered formalin for at least 7 days to
163 kill all pathogens.

164 Viral load measurement (qRT-PCR)

165 Viral loads in swab samples or lung tissue were determined by qRT-PCR. Viral RNA
166 was extracted from swab samples or homogenized tissues using a High Pure Viral RNA

167 Kit (Roche, Germany). Reverse transcription and TaqMan quantitative PCR were
168 performed using a probe one-step real-time quantitative PCR kit (TOYOBO, Japan) on
169 an ABI 7500 Real-Time PCR System. Primers and probes were specific for the gene
170 encoding SARS-CoV-2 N, as follows: F: 5'- GGGGAACTTCTCCTGCTAGAAT -3',
171 R: 5'- CAGACATTTTGCTCTCAAGCTG -3'; probe: 5'-FAM-
172 TTGCTGCTGCTTGACAGATT-TAMRA -3'). The 20 μl reaction mixtures were set up
173 with 8 μl of total RNA. The cycling conditions were as follows: 50°C for 15 min, 95°C
174 for 10 s, and 40 cycles of 95°C for 5 s and 60°C for 30 s. The dilution of each test run
175 refers to the SARS-CoV-2 RNA Reference material (National Institute of Metrology,
176 China). Finally, the copy number of each sample was calculated. Serial dilutions of
177 RNA standards were included with each qRT-PCR to create a standard curve. Viral
178 loads were expressed for the RNA Log dilutions as viral copies/g or copies/ml after
179 calculation with the standard curve. The limit of detection was 100 copies/ml.

180 **ELISA**

181 A SARS-CoV-2-RBD-specific ELISA was used to determine endpoint binding
182 antibody titers of vaccine immune serum. Endpoint titers were defined as the reciprocal
183 serum dilution that yielded an OD450 > 2-fold over background values. Briefly, 96-
184 well plates were coated with 10 μg/ml recombinant RBD protein in carbonate-
185 bicarbonate buffer (pH 9.6) at 4°C overnight. The plates were then blocked with 5%
186 skim milk in PBS (pH 7.4) at 37°C for 1 h. Serum specimens were added to the top row
187 (1:100), and 2-fold serial dilutions were tested in the remaining rows. The plates were
188 incubated at 37°C for 1 h, followed by five washes with PBST. Subsequently, the plates

189 were incubated with an HRP-conjugated anti-human IgG antibody working solution at
190 37°C for 30 min and washed with PBST five times. The assay was developed using
191 3,3',5',5-tetramethylbenzidine HRP substrate (TMB) with 100 μl in each well and
192 stopped by the addition of 50 μl of 2 M H_2SO_4 for 10 min. Wells were measured at 450
193 nm by a microplate reader using Softmax Pro 6.0 software (Molecular Devices, CA,
194 USA). All ELISA measurements were repeated at least three times with each sample in
195 triplicate.

196 **Western blotting**

197 Purified recombinant RBD protein was first separated by SDS-PAGE and then
198 electrotransferred to a polyvinylidene difluoride (PVDF) membrane using a semidry
199 blotting apparatus (15 V, 40 min). After transfer, the membranes were blocked with 5%
200 skim milk in TBS buffer containing 0.1% Tween-20 for 2 h at 37°C and rinsed once
201 with PBST. Afterward, the membranes were incubated with primary antibody (rabbit
202 polyclonal antibodies against SARS-CoV-2-S1 at 0.1 μg/ml, prepared in blocking
203 buffer; SinoBiological, Beijing, China). After 1 h of incubation, the membranes were
204 washed five times with TBS containing 0.1% Tween-20, incubated with horseradish
205 peroxidase (HRP)-conjugated goat anti-rabbit IgG (0.1 μg/ml prepared in blocking
206 buffer) as the secondary antibody for one h, and then washed 5 times. Finally, the
207 membranes were detected by an ECL system (CLINX, China).

208 **Neutralization assays**

209 **a) SARS-CoV-2 surrogate virus neutralization test**

210 A surrogate virus neutralization test (sVNT) based on antibody-mediated blockage of

211 ACE2 binding to SARS-CoV-2-RBD was performed on serum specimens using a
212 commercially available SARS-CoV-2 sVNT Kit (L00847; GenScript, Nanjing, China)
213 according to the manufacturer's instructions. The serum specimens and positive or
214 negative controls were diluted with HRP-RBD solution at a volume ratio of 1:1, i.e., 60
215 μl of sample was mixed with 60 μl of HRP-RBD solution. The mixtures were incubated
216 at 37°C for 30 min. Then, 100 μl each of the mixtures was added to the corresponding
217 96-well plate well. The plate was covered with a Plate Sealer and incubated at 37°C for
218 15 min. The plate was washed four times with 260 μl of Wash Solution. Then, 100 μl
219 of TMB solution was added to each well, and the plate was incubated in the dark at 20
220 - 25°C for 15 min. Finally, 50 μL of Stop Solution was added to each well to quench
221 the reaction. The absorbance was immediately read in a microtiter plate reader at 450
222 nm. All measurements were repeated at least three times with each sample in triplicate.

223 **b) Plaque reduction neutralization test**

224 Live SARS-CoV-2 NAb levels were measured with a standard plaque reduction
225 neutralization test (PRNT) in a BSL-3 facility. Briefly, serum specimens were heat-
226 inactivated for 30 min at 56°C, serially diluted 2-fold from 1:25 to 1:12800 with DMEM
227 containing 2% FBS in 96-well microplates, mixed with 50 plaque-forming units (PFU)
228 of the SARS-CoV-2 20SF107 virus strain and incubated for 1 h at 37°C. The virus-
229 serum mixtures were transferred to 12-well plates containing confluent Vero E6 cell
230 monolayers at 37°C and with 5% CO_2 for 1 h, and then, the virus/serum-containing
231 medium was removed, followed by washing with PBST. Then, DMEM containing 2%
232 FBS and 0.5% agarose was added to each well to overlay the cells and incubated for 3

233 days at 37°C. The cells were fixed with 10% formalin and stained with 0.2% crystal
234 violet. Plates were washed with ultrapure water and air-dried, followed by plaque
235 counting. Each sample was assessed in triplicate. The neutralization titer was
236 determined by calculating the reciprocal of the highest dilution ratio of serum
237 (neutralization endpoint) that protected 50% of cells from infection, which were defined
238 as 50% effective concentration (EC_{50}).

239 **c) Pseudovirus neutralization test**

240 A lentiviral vector pseudoneutralization test (LVV-PsN) based on antibody-mediated
241 blockage of pseudovirus infection of cells containing SARS-CoV-2 receptors was
242 performed on serum specimens using two commercially available SARS-CoV-2 LVV-
243 PsN Kit (SC2087A; SC2087L; GenScript, Nanjing, China) according to
244 the manufacturer's instructions. Pseudoviruses bearing the SARS-CoV-2-S protein
245 from the original Wuhan-Hu-1 strain (WT) or the 501Y.V2 (B.1.351) variant were
246 preincubated with serially diluted positive control or serum specimens for 1 h at room
247 temperature, and then virus-antibody mixtures (50 μl) were added to Opti-
248 HEK293/hACE2 cells (50 μl) in a 96-well plate. After 24 h of incubation, another 50
249 μl of fresh DMEM was added to each well of the 96-well plate. The culture medium
250 was discarded 48 h later, and then the cells were incubated with fresh luciferase assay
251 substrate (Promega) for 3~5 minutes at room temperature. The fluorescence signal was
252 detected by a multimode plate reader. Luminescence readout data were normalized to
253 those derived from cells infected with SARS-CoV-2 pseudoviruses. The neutralization
254 titer was determined by reducing the relative luciferase units (RLU) compared with

negative control. The half-maximal inhibitory concentration (NT_{50}) is calculated using nonlinear regression for the tested samples. Before experiments, serum specimens were incubated at 56°C for 30 min to inactivate the complement.

ELISPOT

SARS-CoV-2-specific T cell responses in rhesus macaque PBMCs were assessed by an IFN-γ ELISPOT assay using recombinant SARS-CoV-2 S1 protein (GenScript, Nanjing, China). Ninety-six-well plates (Millipore) were coated with 100 μl of 10 μg/ml anti-human IFN-γ antibody (BD Biosciences, USA) per well overnight at 4°C, blocked for 1 h with sterile PBST containing 5% FBS at 37°C, and washed three times with sterile PBST. PBMCs were resuspended to 2×10^5 cells/ml in RPMI 1640 medium with 10% heat-inactivated FBS (Invitrogen) and then added to the plate and subsequently stimulated with S1 protein (2 μg/ml in each well), concanavalin A (10 mM) as the positive control, and RPMI 1640 medium as the negative control. Following 20 h of incubation at 37°C, the plates were washed five times with sterile PBST and distilled water. The plates were then incubated with 2 μg/ml biotinylated anti-human IFNγ antibody for 1 h at room temperature, washed six times with sterile PBST, and incubated for 1 h at room temperature with streptavidin–HRP. After five washes with sterile PBST and one with sterile PBS, AEC substrate solution (Abcam) was added to the plates. When the spots were clear enough, the reaction was stopped by washing with distilled water and air-dried, and spots were counted with an ELISPOT Analysis System (At-Spot-2100, China). Assays of all specimens were performed in triplicate. Cells

277 alone in the absence of stimulants were used as a negative control. The numbers of spot-
278 forming cells (SFCs) per 10^6 cells were calculated. The medium background levels
279 were typically < 15 SFC per 10^6 cells.

280 ICS and flow cytometry

281 SARS-CoV-2-specific $CD4^+$ and $CD8^+$ T cell responses in NHP PBMCs were assessed
282 by flow cytometry using recombinant SARS-CoV-2 S1 protein (GenScript, Nanjing,
283 China). Briefly, NHP PBMCs were added to a plate (1×10^6/well) and then stimulated
284 with S1 protein (2 μg/ml in each well) or RPMI 1640 medium as a control for 5 h.
285 Subsequently, the cells were incubated with GolgiPlug/GolgiStop (BD Biosciences,
286 USA) to block intracellular cytokine transport for 6 h at 37°C. Afterward, the cells were
287 washed and surface stained with antibodies against human CD4 (FITC-conjugated),
288 CD8α (FITC-conjugated), and CD44 (FITC-conjugated) for 30 min at room
289 temperature. Subsequently, cells were fixed and permeabilized with a
290 Cytofix/Cytoperm kit (BD Biosciences, USA). Cells were then washed and incubated
291 with anti-human IFN-γ antibodies (PE-conjugated) for 1 h at room temperature, washed
292 with permeabilization buffer, and fixed in 1% paraformaldehyde. All specimens were
293 processed with a FACSCanton flow cytometer (BD Biosciences, USA).

294 Histopathological analysis

295 Lung tissues were fixed overnight in 4% paraformaldehyde (PFA), dehydrated, and
296 embedded in paraffin. Subsequently, 5-μm-thick tissue sections were processed for
297 histology by hematoxylin and eosin staining as previously described. The

immunohistochemical reaction was performed on paraffin-embedded lung sections using a rabbit anti-SARS-CoV-2-NP monoclonal antibody followed by an HRP-conjugated goat anti-rabbit secondary antibody as described. After the DAB chromogenic reaction, nuclear counterstaining, dehydration and mounting, tissue staining was visualized under a microscope, and images were acquired and analyzed.

Statistical analysis

All statistical analyses were performed using GraphPad Prism 8.0 software (GraphPad Software, CA, USA). Statistical significance among different groups was determined by Student's t-test, and differences between the experimental groups were considered statistically significant at the $P<0.05$ level.

Results

Construction of a SARS-CoV-2 RBD trimer vaccine

To simulate the native SARS-CoV-2 S protein trimeric form and improve conformational homogeneity, a natural trimerization domain of T4 bacteriophage fibritin (foldon) was fused to the C-terminus of the SARS-CoV-2 RBD protein (Fig. 1A). An interleukin-10 signal peptide was added to the N-terminus of the RBD to improve peptide secretion. The recombinant protein, named RBD-trimer, was ectopically expressed in human embryonic kidney (HEK293) cells. RBD-trimer was purified by Ni-NTA affinity chromatography and gel filtration. The purity of the recombinant protein was assessed by SDS-PAGE (Fig. 1B) and Western blot (Fig. 1C)

assays with or without reducing conditions. Notably, RBD-trimer did not dissociate into monomers with heating, indicating the thermal stability of this protein complex. According to the N-terminal sequencing of RBD-trimer, the interleukin-10 signal peptide was efficiently cleaved off. We chose the AddaVax adjuvant, an MF59-like nanoemulsion, to prepare our vaccine formulation to better stimulate cellular immune responses. The AddaVax-adjuvanted RBD-trimer protein was used throughout the following immunizations in animals.

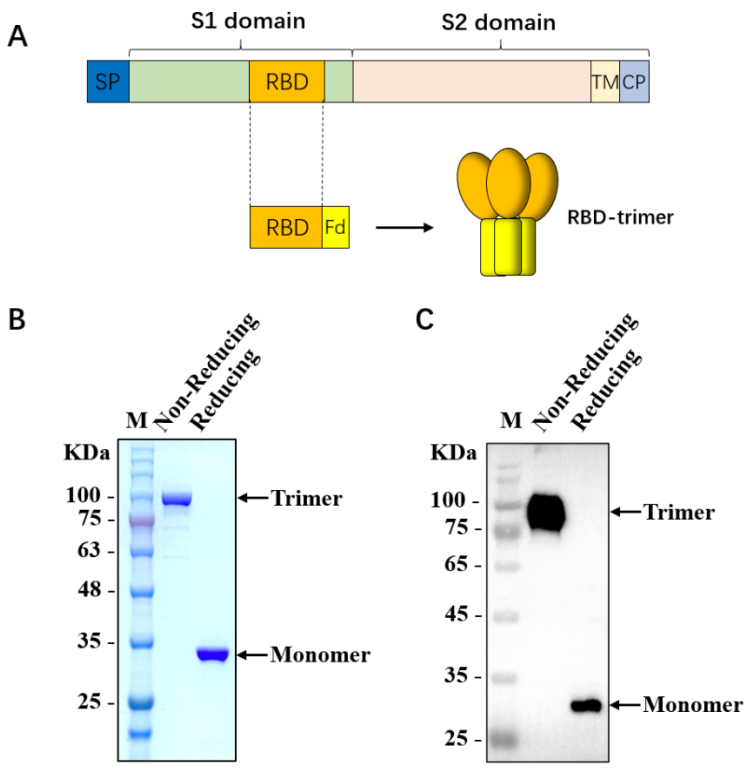

Fig. 1. Characterization of SARS-CoV-2 RBD-trimer.

(A)Schematic design of SARS-CoV-2 RBD-trimer. (B-C) The purified recombinant protein was analyzed by SDS-PAGE (B) and Western blot with a polyclonal antibody against SARS-CoV-2-S1 (C). M: Marker. 10 μg of recombinant protein was loaded in

each lane.

335 **Immunization with RBD-trimer elicited robust humoral and cellular**
336 **immune responses in *rhesus macaques***

337 To assess the immunogenicity of the SARS-CoV-2 RBD-trimer vaccine, five male
338 *rhesus macaques* (3-6 years old) were vaccinated with either RBD-trimer or
339 phosphate-buffered saline (PBS). The animals were intramuscularly immunized with
340 50 μg of RBD-trimer with AddaVax adjuvant (n=3, animal numbers: #140829, #140271,
341 #163957) or PBS (n=2, animal numbers: # 17361, #17321) at 0, 3 and 21 weeks. All
342 the macaques were phlebotomized as outlined in Fig. 2A. Serum was isolated for
343 ELISA and neutralizing activity tests, in which NAbs were measured by a standard
344 plaque-reduction neutralization test (PRNT), a lentiviral vector pseudoneutralization
345 test (LVV-PsN), and a surrogate virus neutralization test (sVNT) based on antibody-
346 mediated blockage of ACE2 binding to the RBD. The NAb average titers of the
347 vaccinated animals reached approximately 100 (EC_{50})/200 (sVNT) and 1000
348 (EC_{50})/4000 (sVNT) after the first and second immunizations, respectively, and then
349 gradually decreased to 130 (EC_{50})/400 (sVNT) at week 21. Considering a previous
350 report that NAbs can achieve full immune protection as long as the titer reaches 50
351 (EC_{50}) [5], these data suggest that our RBD-trimer vaccine can induce acute and durable
352 protective immunity for no less than 4 months in macaques. The second boost produced
353 extremely high titers of NAbs (2600 EC_{50}, 8000 sVNT) (Fig. 2B, C and Fig. S1A).
354 Similar to the NAb results, RBD-specific ELISA IgG titers in the vaccination group
355 gradually increased and peaked after the boosts (Fig. 2D). To evaluate whether the
356 501Y.V2 variant is resistant to neutralization by RBD-trimer vaccinee serum, we tested

357 the neutralizing activity against the original SARS-CoV-2 strain (WT) and 501Y.V2
358 variant on day 7 post-second boost using the LVV-PsN assay, and the results showed
359 that the NAb average titer was approximately 1030 (NT_{50}) against the 501Y.V2 variant,
360 which is approximately 30% lower than that against the WT strain (NT_{50} of 1500) (Fig.
361 2E and Fig. S1B). By contrast, the neutralizing activities of mRNA vaccinee serum
362 against the 501Y.V2 variant were significantly lower (41.2-fold reduction, Pfizer; 20.8-
363 fold reduction, Moderna) [25, 26], suggesting that our vaccine can protect against
364 infection with the 501Y.V2 variant. Neither RBD-specific binding antibodies nor NAbs
365 were detected in the sham-vaccinated macaques.

366 Peripheral blood mononuclear cells (PBMCs) were isolated after the first booster
367 immunization, and SARS-CoV-2-specific CD4+ and CD8+ peripheral blood T cell
368 responses were measured by IFN-γ enzyme-linked immunospot (ELISPOT) and
369 intracellular cytokine staining (ICS) assays. Compared to that of the sham group, IFN-
370 γ secreted by PBMCs was significantly increased after SARS-CoV-2-S1 stimulation
371 (140-440 spots/10^6 cells from 7-21 spots/10^6 cells, Fig. 2F). Moreover, the proportion
372 of IFN-γ-secreting $CD4^+$ T cells (IFN-γ/$CD4^+$) in all $CD4^+$ T cells increased from 0.12%
373 to 0.32-0.44% (Fig. 2G, I), while the proportion of IFN-γ-secreting $CD8^+$ T cells (IFN-
374 γ/$CD8^+$) reached 0.70-90% from 0.18% (Fig. 2H, J), demonstrating that immunization
375 with RBD-trimer stimulated a potent specific cellular immune response.

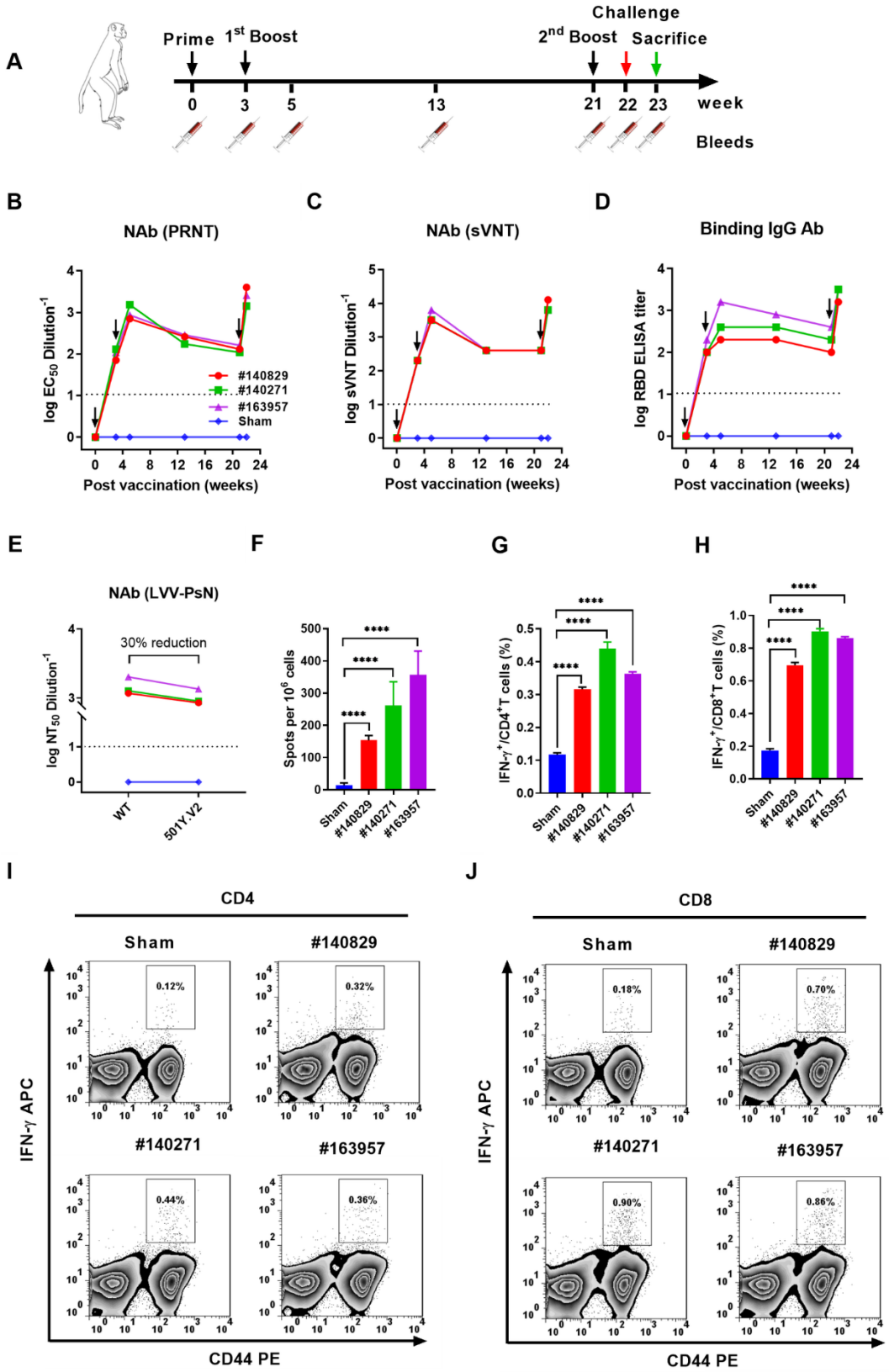

Fig. 2. SARS-CoV-2 RBD-trimer induced robust humoral and cellular immune responses in *rhesus macaques*.

Flow chart of experimental design (A). Arrows indicate weeks of immunization (black), challenge (red), and sacrifice (green), syringes indicate sampling weeks. The serum samples were used to test NAb titers by PRNT assay (B) and a surrogate virus neutralization test (sVNT) (C) and RBD-specific ELISA antibody titers (D). Neutralization of the original Wuhan-Hu-1 (WT) and 501Y.V2 variant viruses by the second-boost serum was measured with the use of a recombinant lentiviral-based pseudovirus neutralization assay (LVV-PsN) (E). Measurements below the detection limit were assigned a value of 1. PBMCs isolated from immunized and sham groups 2 weeks after the first boost were collected for IFN-γ detection by ELISPOT assay after stimulation with S1 protein (F). The proportion (G, I) of $CD4^+$ T cells secreting IFN-γ among all $CD4^+$ T cells and the proportion (H, J) of $CD8^+$ T cells secreting IFN-γ among all $CD8^+$ T cells were evaluated by intracellular cytokine staining. The dotted lines indicate the detection limit. Data are shown as the means ± SEM (standard errors of the mean). *P* values were analyzed by Student's t-test (****, $P < 0.0001$).

395 **The RBD-trimer vaccine provides complete protection against SARS-**
396 **CoV-2 challenge in *rhesus macaques***

397 We next assessed the protective efficacy of the RBD-trimer vaccine against SARS-
398 CoV-2 infection in *R. macaques*; all the macaques were intranasally and tracheally
399 challenged with 1×10^7 $TCID_{50}$ of the SARS-CoV-2 20SF107 strain at 9 days after the
400 second booster vaccination (Fig. 2A). Throat, nose, and rectal swabs and tracheal brush
401 specimens were collected over a time course post-infection. All animals were
402 euthanized at 7 days post-infection (dpi) to assess the viral load in the respiratory tissues.
403 A high virus burden was detected in the swab specimens from the throat, nose, and
404 rectum and tracheal brushes throughout the control animals' detection periods (Fig. 3
405 A, B, C, D). The virus loads in nasal swabs and tracheal brushes of control macaques
406 gradually decreased after reaching peak values at 2 dpi. In comparison, the virus loads
407 in anal swabs increased gradually from 2 dpi. In contrast, a mild viral infection was
408 detected in the swabs and tracheal brushes at 1 dpi and then quickly dropped to an
409 extremely low level in the RBD-trimer-immunized macaques. All seven different lung
410 lobe tissues from the control macaques showed high levels of viral genomic RNA. In
411 contrast, no viral RNA was detected in the immunized macaques, indicating that our
412 RBD vaccine candidate could confer sterilizing immunity in lung tissues (Fig. 3E).
413 Additionally, no clinical signs were found in the immunized macaques after challenge,
414 while the control macaques exhibited symptoms, including cough and increased body
415 temperature (Fig. 3F).

416

417 Histopathological analysis of the fixed lungs was performed with hematoxylin-
418 eosin (H&E) staining. No visible pathological change or inflammatory cell infiltration
419 was observed in the lung tissues from immunized macaques (Fig. 4A, B). In contrast,
420 severe histopathological changes were found in the control macaques, including
421 apparent thickened alveolar walls, mononuclear inflammatory cell infiltration, focal
422 exudation, hemorrhage, and architecture disappearance (Fig. 4C, D).
423 Immunohistochemical (IHC) assays indicated that multiple pneumocytes in the lung
424 sections from the control macaques were positive for SARS-CoV-2 N protein staining
425 (Fig. 4G, H). By contrast, no viral antigen was detected in the lung tissues from the
426 immunized animals (Fig. 4E, F).

427

428

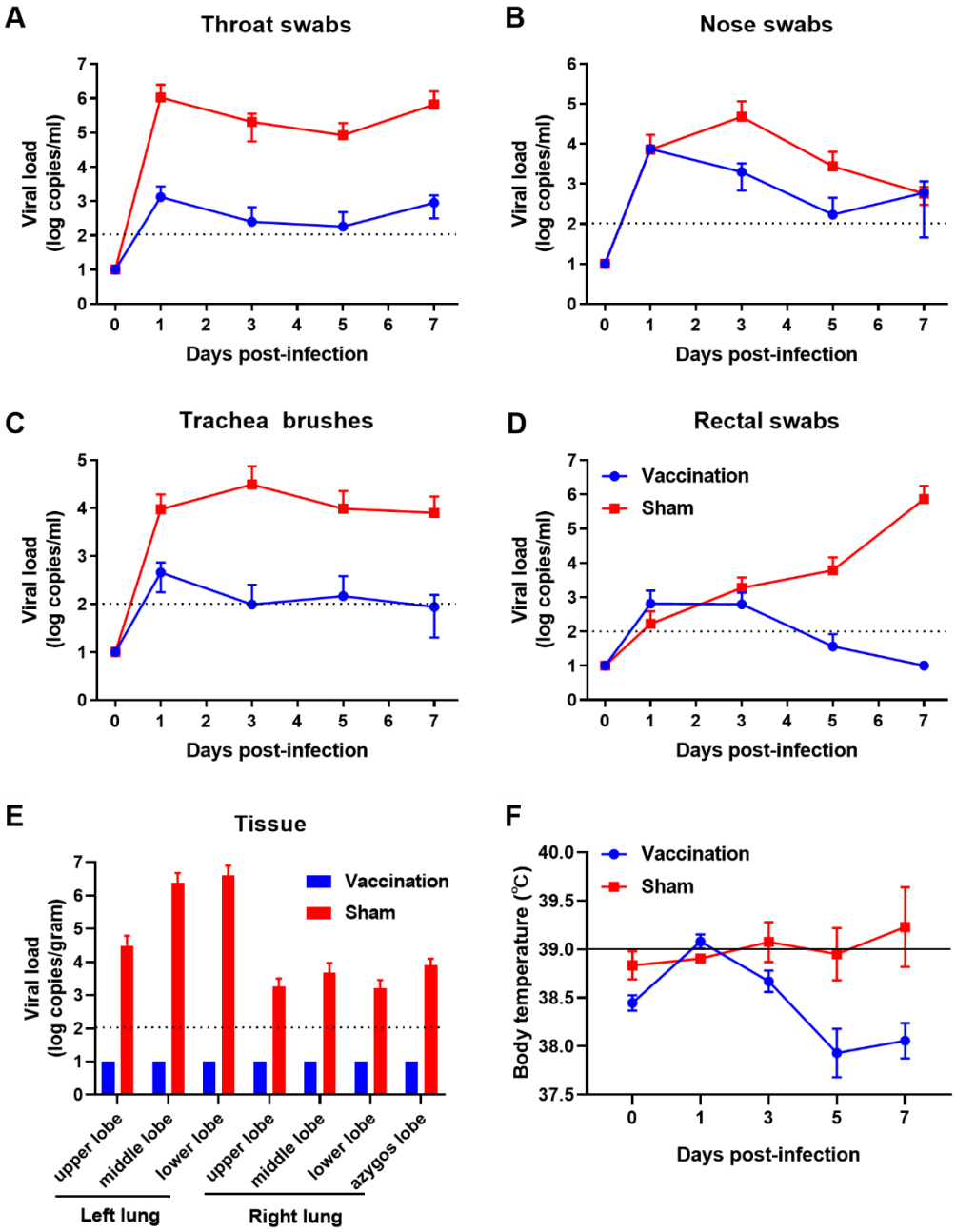

Fig. 3. Protective efficacy of the RBD-trimer vaccine in *rhesus macaques*.

Macaques were challenged intranasally and tracheally with SARS-CoV-2. Viral loads in throat swabs (A), nasal swabs (B), tracheal brushes (C), rectal swabs (D), and lung tissues (E) were measured by qRT-PCR. Changes in body temperature of the animals (F). The dotted lines indicate the detection limit. Measurements below the limit of detection were assigned a value of 10. The solid lines represent the upper limit of the

standard body temperature reference value.

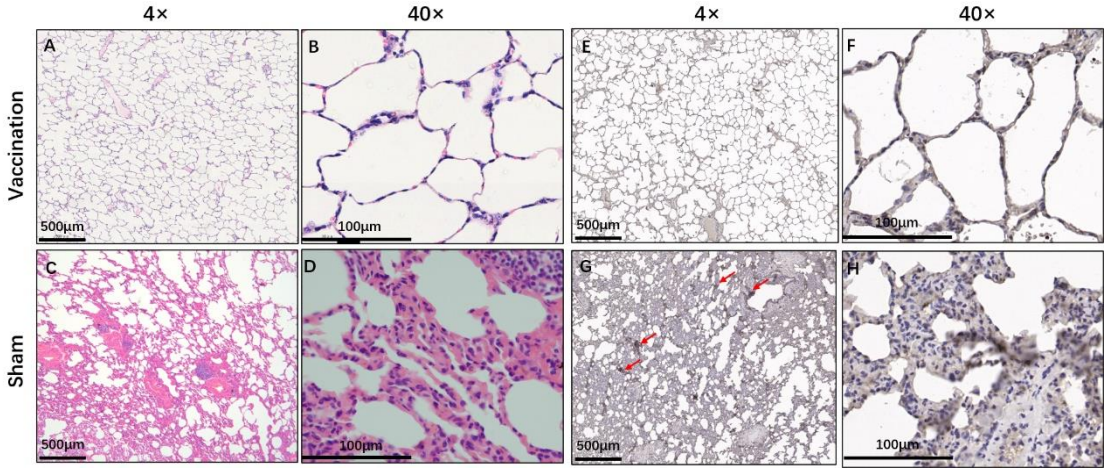

Fig. 4. H&E staining and IHC analysis of lungs from rhesus *macaques*

Macaques immunized with RBD-trimer or PBS were sacrificed at 7 dpi. Lung tissue sections were stained by H&E staining (A, B, C, D). IHC detection of the N protein of SARS-CoV-2 (E, F, G, H). Immunohistochemically positive cells are marked by red arrows. Images of different tissue pathologies at low magnification (4×) and higher magnification (40×) are shown.

To evaluate anamnestic humoral and T cell responses in vaccinated *rhesus macaques* after challenge, paired serum and PBMCs were collected from vaccinated animals before and after SARS-CoV-2 challenge, and changes in the NAb titer and the percentage of cytokine-expressing CD4+ and CD8+ T cells were analyzed. The results showed that the NAb titer did not change one week after viral challenge, indicating that no anamnestic humoral immune response was induced. When the vaccine candidate fails to induce a sufficient protective immune response [11], the challenge enhances NAb titers; therefore, our vaccine protection is sterilizing. Simultaneously, the proportions of CD4 and CD8 T cells secreting IFN-γ, IL-2, IL-4 and TNF-α increased significantly (approximately 1.5-fold or 2.5-fold increase in CD4 or CD8 T cells), suggesting that the SARS-CoV-2-specific memory T cell immune response was stimulated to secrete cytokines.

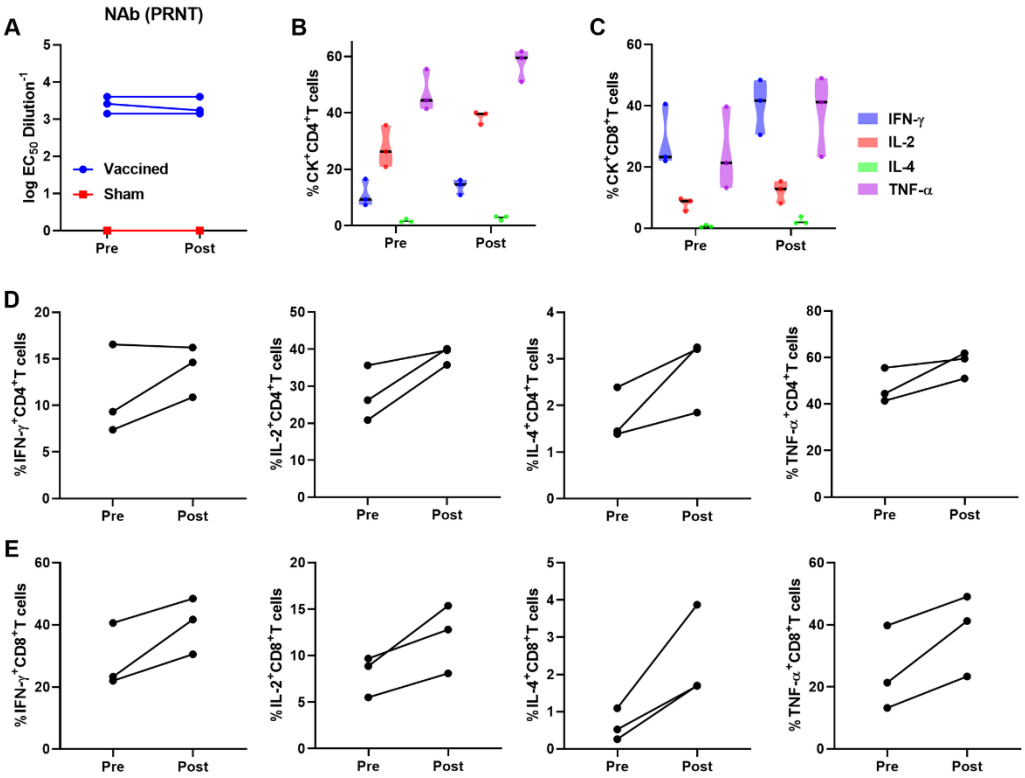

Fig. 5. NAb and memory T cell responses induced by SARS-CoV-2 infection in vaccinated *rhesus macaques*

Serum and PBMCs were collected and isolated from macaques before infection (Pre) and 7 dpi (Post). Serum NAb titers were measured by PRNT assay (A). Cells were stained for intracellular production of IFN-γ, IL-2 IL-4 and TNF-α. The grouped violin plot graphs show the mean changes in the total percentage of CD4+ and CD8+ T cells expressing the indicated cytokine in the blood (B, C). Each line represents an individual animal (D, E).

469 Hematology and serum biochemistry values of all macaques were tested over a time
470 course post-infection. The number of platelets in the control macaques increased and
471 reached a peak at 5 dpi, indicating hemorrhage in the tissues (Fig. S2), which suggested
472 blood cell exudation in the lung blood vessels. In addition, the number of lymphocytes
473 in the control macaques slightly increased. The concentrations of aspartate
474 aminotransferase (AST) and alanine aminotransferase (ALT) in the serum of the control
475 macaques increased and exceeded the upper reference range at 1 and 2 dpi, suggesting
476 that these macaques had liver injury after SARS-CoV-2 challenge (Fig. S3). By contrast,
477 the hematological and biochemical states of immunized macaques stayed at a normal
478 range during the viral challenge periods.

479 Compared with young people, the frail middle-aged population has higher risks of
480 severe COVID-19 with a higher mortality rate, and the virus replicates more efficiently
481 in their lungs and other organs[28]. NHP model animals infected with SARS-CoV-2
482 showed that older macaques developed extreme viral replication in the lungs[29].
483 Therefore, the protective effect of vaccines for middle-aged and frail people is highly
484 valuable. Thus, our vaccination group included a frail macaque (#140829, 6 years old,
485 4.8 kg), which was only half the weight of macaques of the same age. This animal can
486 better simulate the candidate vaccine's immune and protective efficacy for frail people.
487 Compared to the other two macaques, this animal had a slightly weaker immune
488 response and lower antibody levels during the first 2 vaccinations. However, after the
489 third immunization, its immune responses were no different from those of the other
490 macaques (Fig. 2B, C and Fig. S1A). This frail monkey was fully protected by RBD-

trimer vaccination, suggesting that the vaccine could provide adequate protection to middle-aged and frail people against COVID-19.

Discussion

The severe COVID-19 pandemic and the precipitously increasing numbers of deaths worldwide necessitate the urgent development of SARS-CoV-2 vaccines. Global researchers are racing toward safe and effective vaccines against COVID-19 based on multiple platforms, and some vaccines have received emergency use validation, including mRNA vaccines (Moderna, Pfizer/BioNTech), inactivated virus vaccines (Sinopharm, Sinovac, Janssen), and adenovirus vector-based vaccines (AstraZeneca, CanSino). In this study, an engineered trimeric RBD subunit vaccine candidate elicited robust humoral and cellular immune responses in nonhuman primates (NHPs), resulting in significant protection against SARS-CoV-2 infection.

To improve the immunogenicity of the recombinant RBD protein and better mimic the native trimeric SARS-CoV-2 S structure, we fused a trimer motif to make the RBD form a stable trimer structure; the construct will not dissociate even if the temperature is above 60°C, and there was no change after 3 months of storage at 4°C. Western blot analysis showed that compared with the monomer, the trimer binds to the SARS-CoV-2 S1 polyclonal antibody more strongly, suggesting that the conformational epitope is better retained. In contrast with the results of other vaccine candidates reported in the NHP model [5], NHPs can obtain protective NAb titers (EC_{50} titer of 100) with a single dose of our candidate, suggesting that it can be used for emergency vaccination of high-

risk populations. There are few reports about the persistence of NAb responses induced by COVID-19 vaccine candidates. To evaluate the candidate's protection persistence, our immunity cycle spanned half a year. The results showed that the antibody level gradually decreased to an EC_{50} average titer of 50 4 months after the second vaccination. Although the antibody level was much lower than that immediately after vaccination, it was still above the protective antibody level, suggesting that this vaccine can achieve no less than 4 months of long-lasting humoral protection. Considering that SARS-CoV-2 may coexist with humans for a long time, a vaccine that can generate acute and durable immune protection is of great value. Due to the high variability of SARS-CoV-2, multiple variants have recently been identified and are now spreading worldwide, such as B.1.1.7 (501Y.V1), B.1.351 (N501Y.V2) and P1 (N501Y.V3), which appear to be more easily transmitted [30]. There is a growing concern that the N501Y.V2 and N501Y.V3 variants could impair the protective efficacy of licensed vaccines [26]. Therefore, the broad-spectrum protection of the vaccine is also a focus of our attention. Previous research reported that the AddaVax adjuvant, a squalene-based oil-in-water emulsion similar to MF59, could increase the broad protection of the influenza virus vaccine by stimulating a cross-protective humoral response [31]. Compared with aluminum adjuvants, squalene-based adjuvants have been shown to induce humoral and cellular immune responses in a more balanced manner [32]. Therefore, we chose this adjuvant to formulate our candidate vaccine. Excitingly, the antibodies produced in response to our vaccine showed good neutralizing activity against N501Y.V2 variant.

NAbs are considered to play a vital role in preventing SARS-CoV-2 infections. Monoclonal antibodies (MAbs) and convalescent plasma have been used to treat severe COVID-19 and have shown sound therapeutic effects. A MAb regimen has been authorized by the US Food and Drug Administration to treat COVID-19. Therefore, the NAb titer induced by a vaccine is a crucial parameter for vaccine development. The cellular immune response is also a critical effector in virus clearance and alleviation of clinical symptoms. Moreover, studies have shown that the duration of the memory T cell response induced by infection is much longer than that of antibody levels, so cellular immunity plays a crucial role in the durability of vaccine protection [33]. In addition, as the level of NAbs gradually decreases after vaccination, nonneutralizing antibodies may promote infection via the ADE effect, but virus-specific T cell immunity can reduce this potential risk. An ideal vaccine should be able to induce humoral and cellular immune responses in a balanced manner. Compared with the RBD monomer, RBD-trimer generated a higher level of NAbs, resulting in more potent protection. In addition, it is surprising that by formulating an Addavax adjuvant, our vaccine candidate also demonstrated a strong CD4+ and CD8+ T cell immune response in NHPs, suggesting more robust protection.

SARS-CoV-2 infects hosts mainly in the respiratory tract and lung, and pneumonia is the typical symptom of COVID-19; our data correspond to this report. Sham-immunized macaques showed severe pneumonia; in contrast, macaques immunized with our vaccine candidate exhibited significant protection of the lung with viral clearance. The main changes in sham-immunized macaques were inflammatory

granulocyte infiltration, disseminated thickening of alveolar septa, and hemorrhage. By contrast, immunized macaques showed less severe lung symptoms. Hematological analysis showed that the platelet concentration of the sham-immunized macaques continued to increase and reached a peak at 5 dpi, suggesting visceral bleeding. In contrast, the immunized macaques did not have any hematological abnormalities. Furthermore, no viral RNA was detected in the lungs of the immunized macaques by qPCR or immunohistochemical assays. By contrast, in the lungs of sham-immunized macaques, the viral RNA level reached almost 10^7 copies/gram. These results proved that our vaccine candidate conferred sterilizing immunity in the lung tissue of immunized NHPs. SARS-CoV-2 attacks host organs beyond the lung; liver injury has also been recorded. In this work, after challenge, the ALT and AST values of the unimmunized animals increased, indicating that SARS-CoV-2 attacked their liver. There were no abnormalities in the vaccinated animals, which means that our vaccine candidate may protect the animals from liver injury. In short, our candidate vaccine can effectively protect the organs of NHPs from virus attacks.

Since the antibody level induced by infection or vaccination cannot last overly long, when the antibody level of the population drops to a level insufficient to achieve immune protection, there is a risk of reinfection. Once there is another outbreak, how can individuals quickly obtain immune protection? Our results proved that only one boost could quickly regain complete immune protection for the vaccinated NHPs. Notably, after the COVID-19 pandemic is under control, if SARS-CoV-2 infection appears again, people who have been vaccinated can be immediately administered a

booster immunization to avoid another large-scale outbreak of the epidemic.

Multiple mammalian species, including rats, mice, guinea pigs, rabbits, cynomolgus macaques, and rhesus macaques, have been used for COVID-19 animal models. It is still too early to define the most suitable animal model for studying SARS-CoV-2 infections. Because of their close genetic relation to humans, NHPs are usually used as animal models to evaluate vaccines and drugs against human disease. We provided evidence for trimeric RBD subunit vaccine safety in NHPs and did not observe infection enhancement or immunopathological exacerbation in our studies. Our data also demonstrate significant protection against SARS-CoV-2 challenge with 50 μg per vaccination dose in NHPs.

In summary, our RBD-based subunit vaccine candidate induced robust humoral and cellular immune responses and protected NHPs against SARS-CoV-2 infection, and it also showed perfect safety. There were no abnormalities in body temperature, weight, clinical signs, pathology, hematology, or biochemical indicators during vaccination and challenge. These data proved the possibility that our trimeric RBD can be a promising candidate vaccine to prevent COVID-19.

Conflict of interest

The authors declare that they have no conflict of interest.

Acknowledgments

We thank JFS and JHZ from Beijing Primabio Inc for their assistance with husbandry and experiments. This study was funded by National Key Technologies Research and Development Program grants 2018YFC1200600 and 2018YFC1200500 to LMY. and a grant from Strategic Priority Research Program of Chinese Academy of Sciences XDB29010000 to WJL.

Author contributions

Conceptualization: LMY, WJL; Methodology: LMY, DYT, JBH, WHF; Investigation: LMY, YZ, WQS, YLL, XDT, YQW, DDY, XLF; Visualization: LMY, YHB; Funding acquisition: LMY, WJL; Project administration: WJL, LMY; Supervision: WJL, YTZ; Writing – original draft: LMY, DYT; Writing – review & editing: WJL, YHB, GC

References

[1] Chen N, Zhou M, Dong X, et al. Epidemiological and clinical characteristics of 99 cases of 2019 novel coronavirus pneumonia in wuhan, china: A descriptive study. Lancet 2020; 395: 507-513.

[2] Zhu FC, Li YH, Guan XH, et al. Safety, tolerability, and immunogenicity of a recombinant adenovirus type-5 vectored covid-19 vaccine: A dose-escalation, open-label, non-randomised, first-in-human trial. Lancet 2020; 395: 1845-1854.

[3] Knoll MD, Wonodi C. Oxford-astrazeneca covid-19 vaccine efficacy. Lancet 2021; 397: 72-74.

[4] Mercado NB, Zahn R, Wegmann F, et al. Single-shot ad26 vaccine protects against sars-cov-2 in rhesus macaques. Nature 2020; 586: 583-588.

[5] Gao Q, Bao L, Mao H, et al. Development of an inactivated vaccine candidate for sars-cov-2. Science 2020; 369: 77-81.
[6] Wang H, Zhang Y, Huang B, et al. Development of an inactivated vaccine candidate, bbibp-corv, with potent protection against sars-cov-2. Cell 2020; 182: 713-721 e719.
[7] Smith TRF, Patel A, Ramos S, et al. Immunogenicity of a DNA vaccine candidate for covid-19. Nature communications 2020; 11: 2601.
[8] Yu J, Tostanoski LH, Peter L, et al. DNA vaccine protection against sars-cov-2 in rhesus macaques. Science 2020; 369: 806-811.
[9] Alberer M, Gnad-Vogt U, Hong HS, et al. Safety and immunogenicity of a mrna rabies vaccine in healthy adults: An open-label, non-randomised, prospective, first-in-human phase 1 clinical trial. Lancet 2017; 390: 1511-1520.
[10] Corbett KS, Flynn B, Foulds KE, et al. Evaluation of the mrna-1273 vaccine against sars-cov-2 in nonhuman primates. The New England journal of medicine 2020; 383: 1544-1555.
[11] Zhang NN, Li XF, Deng YQ, et al. A thermostable mrna vaccine against covid-19. Cell 2020; 182: 1271-1283 e1216.
[12] Yang J, Wang W, Chen Z, et al. A vaccine targeting the rbd of the s protein of sars-cov-2 induces protective immunity. Nature 2020; 586: 572-577.
[13] Dai L, Zheng T, Xu K, et al. A universal design of betacoronavirus vaccines against covid-19, mers, and sars. Cell 2020; 182: 722-733 e711.
[14] Ghorbani A, Zare F, Sazegari S, et al. Development of a novel platform of virus-like particle (vlp)-based vaccine against covid-19 by exposing epitopes: An immunoinformatics approach. New Microbes New Infect 2020; 38: 100786.
[15] Cai Y, Zhang J, Xiao T, et al. Distinct conformational states of sars-cov-2 spike protein. Science 2020; 369: 1586-1592.
[16] Richmond P, Hatchuel L, Dong M, et al. Safety and immunogenicity of s-trimer (scb-2019), a protein subunit vaccine candidate for covid-19 in healthy adults: A phase 1, randomised, double-blind, placebo-controlled trial. Lancet 2021; 397: 682-694.
[17] Liu L, Wei Q, Lin Q, et al. Anti-spike igg causes severe acute lung injury by skewing macrophage responses during acute sars-cov infection. JCI Insight 2019; 4:
[18] Wan Y, Shang J, Sun S, et al. Molecular mechanism for antibody-dependent enhancement of coronavirus entry. Journal of virology 2020; 94:
[19] Lee WS, Wheatley AK, Kent SJ, et al. Antibody-dependent enhancement and sars-cov-2 vaccines and therapies. Nat Microbiol 2020; 5: 1185-1191.
[20] Walls AC, Fiala B, Schafer A, et al. Elicitation of potent neutralizing antibody responses by designed protein nanoparticle vaccines for sars-cov-2. Cell 2020; 183: 1367-1382 e1317.
[21] Shi R, Shan C, Duan X, et al. A human neutralizing antibody targets the receptor-binding site of sars-cov-2. Nature 2020; 584: 120-124.
[22] Robbiani DF, Gaebler C, Muecksch F, et al. Convergent antibody responses to sars-cov-2 in convalescent individuals. Nature 2020; 584: 437-442.
[23] Marot S, Malet I, Leducq V, et al. Rapid decline of neutralizing antibodies against sars-cov-2 among infected healthcare workers. Nature communications 2021; 12: 844.
[24] Edridge AWD, Kaczorowska J, Hoste ACR, et al. Seasonal coronavirus protective immunity is short-lasting. Nature medicine 2020; 26: 1691-1693.
[25] Wu K, Werner AP, Koch M, et al. Serum neutralizing activity elicited by mrna-1273 vaccine -

663 preliminary report. The New England journal of medicine 2021;
664 [26] Garcia-Beltran WF, Lam EC, St Denis K, et al. Multiple sars-cov-2 variants escape
665 neutralization by vaccine-induced humoral immunity. Cell 2021;
666 [27] Wang P, Nair MS, Liu L, et al. Antibody resistance of sars-cov-2 variants b.1.351 and b.1.1.7.
667 Nature 2021;
668 [28] Shi M, Chen L, Yang Y, et al. Analysis of clinical features and outcomes of 161 patients with
669 severe and critical covid-19: A multicenter descriptive study. Journal of clinical laboratory analysis
670 2020; 34: e23415.
671 [29] Yu P, Qi F, Xu Y, et al. Age-related rhesus macaque models of covid-19. Animal Model Exp
672 Med 2020; 3: 93-97.
673 [30] The L. Genomic sequencing in pandemics. Lancet 2021; 397: 445.
674 [31] Goff PH, Eggink D, Seibert CW, et al. Adjuvants and immunization strategies to induce
675 influenza virus hemagglutinin stalk antibodies. PloS one 2013; 8: e79194.
676 [32] Zhang N, Channappanavar R, Ma C, et al. Identification of an ideal adjuvant for receptor-
677 binding domain-based subunit vaccines against middle east respiratory syndrome coronavirus.
678 Cellular & molecular immunology 2016; 13: 180-190.
679 [33] Zhao J, Alshukairi AN, Baharoon SA, et al. Recovery from the middle east respiratory
680 syndrome is associated with antibody and t-cell responses. Sci Immunol 2017; 2: eaan5393.
681
682

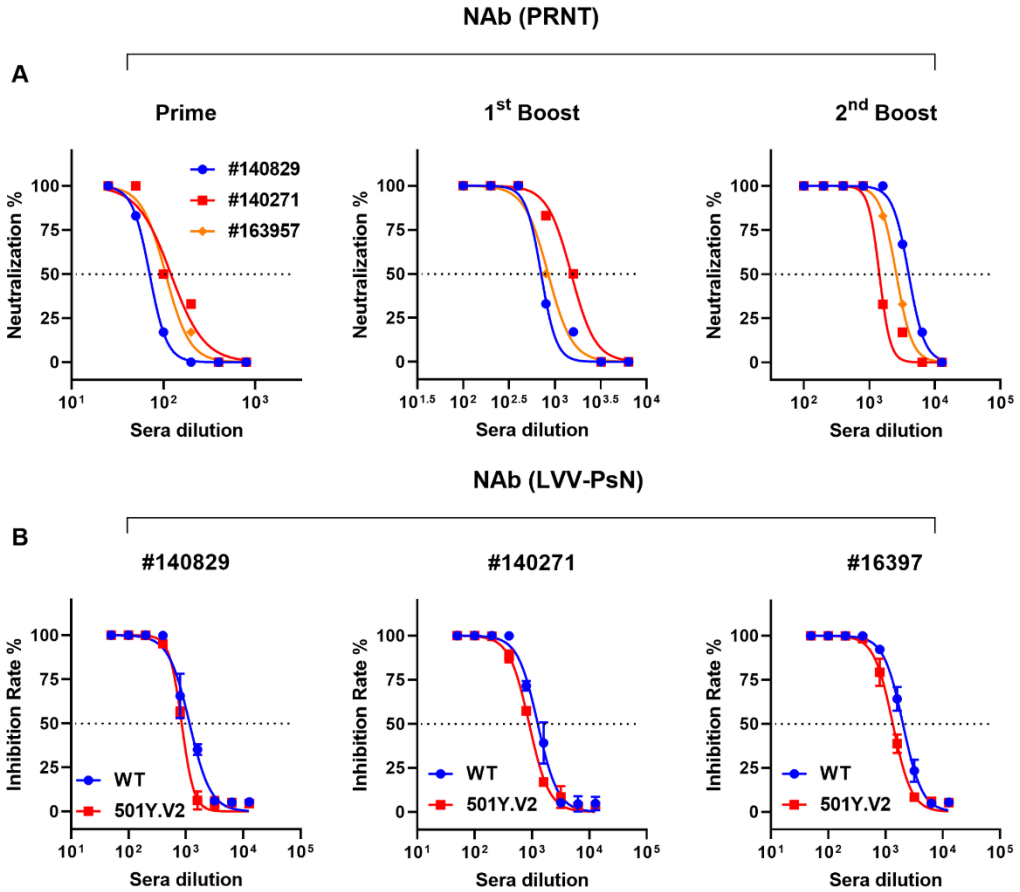

Fig. S1. *In vitro* neutralization assays of immunized *rhesus macaque* serum.

The serum samples after three immunizations were used for testing NAb titers by PRNT assay (A), respectively. The sera samples collected on day 7 post the 2nd boost were used for testing NAb titers by LVV-PsN assay (B). Serial dilutions of serum were pre-incubated with Pseudoviruses bearing the SARS-CoV-2-S protein from the original Wuhan-Hu-1 strain (WT) or the 501Y.V2 (B.1.351) variant, and the percentage inhibition of cell infection were determined. Nonlinear regression was performed using a log (inhibitor) versus normalized response curve and a variable slope model (R2> 0.95 for all curves). The EC_{50} (PRNT) and NT_{50} (LVV-PsN) were calculated by using the Reed-Muench method. Data are shown as means ± SEM.

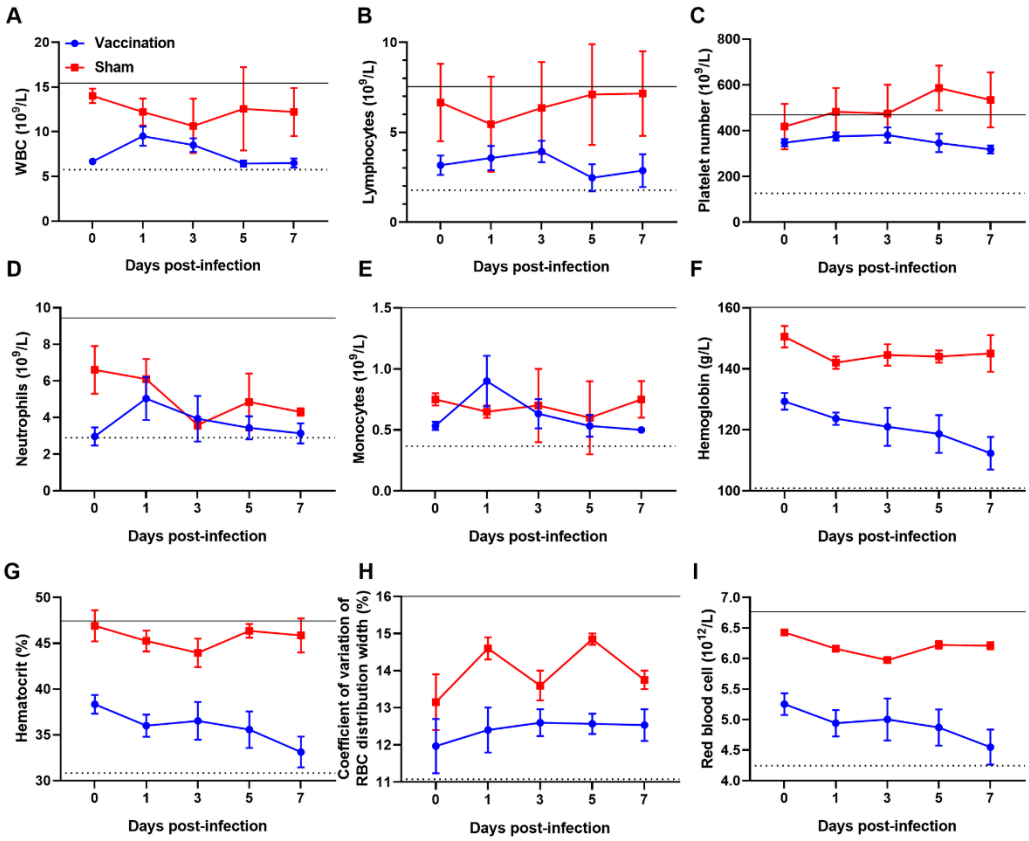

Fig. S2. Hematological index changes of rhesus macaques after SARS-CoV-2 infection.

Macaques were challenged, and hematological values were obtained before and 1, 3, 5, and 7 days after challenge. The solid lines and the dotted lines represent the upper and lower limits of the normal reference range.

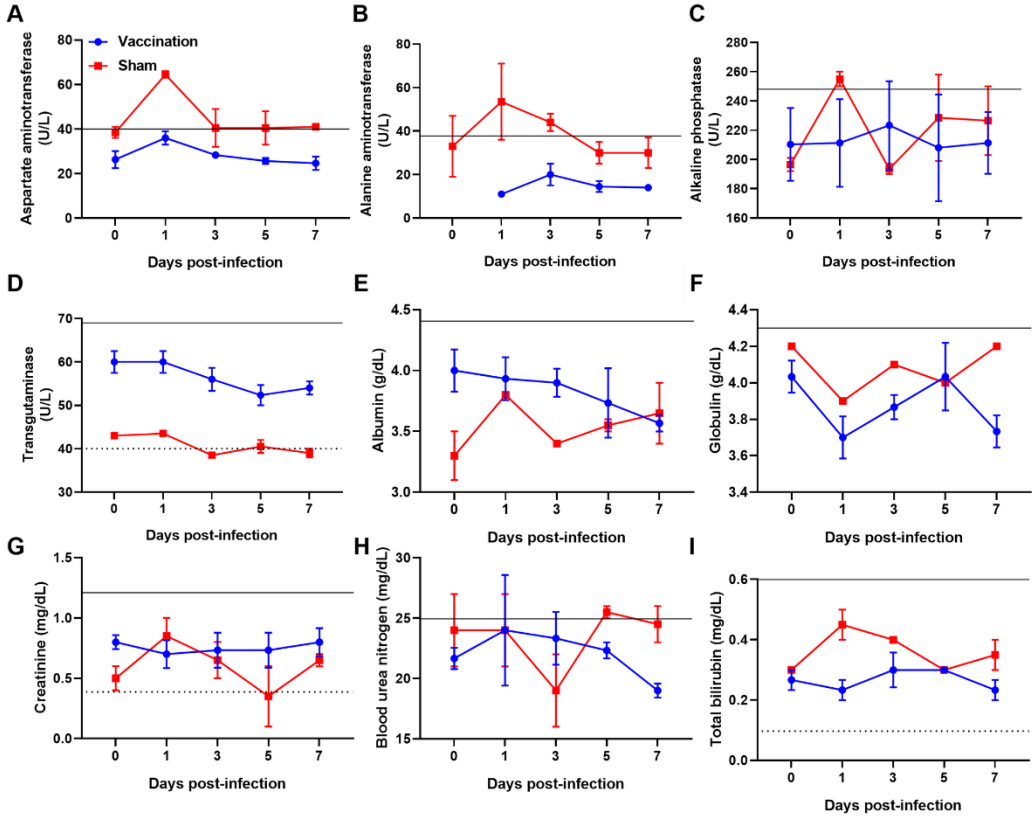

Fig. S3. Serum biochemical index changes of rhesus macaques after SARS-CoV-2 infection.

Macaques were challenged, and body temperature and serum biochemical values were measured before and 1, 3, 5, and 7 days after the challenge. The solid lines and the dotted lines represent the upper and lower limits of the normal reference range.